Northumbria Research Link

Northumbria University NEWCASTLE

IEEE Access
Multidisciplinary : Rapid Review : Open Access Journal

Date of publication xxxx 00, 0000, date of current version xxxx 00, 0000.

Digital Object Identifier 10.1109/ACCESS. 2017.Doi Number

Performance Analysis and Software-Defined Implementation of Real-Time MIMO FSO with Adaptive Switching in GNU Radio Platform

Zun Htay[1, *], Zabih Ghassemlooy[1], Mojtaba Mansour Abadi[1], Andrew Burton[2], Nithin Mohan[1], and Stanislav Zvanovec[3]

[1]Optical Communications Research Group, Faculty of Engineering and Environment, Northumbria University, Newcastle upon Tyne NE1 8ST, UK.
[2]Isocom Limited, 2 Fern Court, Bracken Hill Business Park, Peterlee, SR8 2RR, UK.
[3]Department of Electromagnetic Field, Faculty of Electrical Engineering, Czech Technical University in Prague, 16627 Prague, Czech Republic.

Corresponding author: Zun Htay (e-mail: zun.htay@northumbria.ac.uk).

This work is partly funded by Isocom Limited and intensive industrial innovation program (IIIP) northeast, United Kingdom - 25R17P01847, by the European regional development fund (ERDF), and by the European Union COST Action CA19111 NEWFOCUS.

ABSTRACT: In this paper, we provide the first software-based implementation of multiple-input multiple-output (MIMO) free space optical (FSO) link with the adaptive switching based on the software defined radio developed by GNU Radio software system, which emulates the real-time capability of the proposed scheme. We propose a switching mechanism to independently configure each transmitter and receiver, based on the channel state information provided at the transmitter via a feedback link and evaluate the link performance under atmospheric conditions such as fog and turbulence. We also validate the advantages of mitigating both the turbulence and fog in the proposed MIMO FSO system by means of numerical simulations and the developed GNU Radio software platform.

INDEX TERMS FSO; MIMO; software defined radio; GNU Radio; Adaptive switching; Fog; Turbulence.

I. INTRODUCTION

Over the next decade, the number of smart devices to be connected is expected to double, and consequently, the data traffic generated is predicted to increase a thousandfold [1]. This rapid expansion of data generated will impose noticeable pressure on the bandwidth usage of current wireless networks. Therefore, the fifth and sixth generations (5G and 6G) wireless technologies are aiming to address the connectivity challenges associated with the future Internet of things (IoT) including people-to-devices communications, device-to-device communications, etc. by utilizing the emerging machine learning on a grand scale. As part of the 5G and 6G, to meet the spectrum congestion and ensure reliable connectivity with 99.999% link availability, the optical wireless communications (OWC) has been considered [1, 2]. OWC offers several advantages including a virtually unlimited licensed free bandwidth in the infrared band when compared to the overcrowded radio frequency (RF) spectrum, inherent security at the physical layer by confining the optical beams in restricted areas, optical fibre type high data rates, etc. could be adopted in certain applications, where RF-based systems cannot be effectively utilized [1]. As a branch of OWC, the free space optical (FSO) systems have been deployed in short to long haul transmission links including the last-mile/meter access networks, building-to-building communications, video surveillance, broadcasting, and satellite-to-satellite communications, to name a few [1, 3, 4].

While the aforementioned examples probed the realistic applications of FSO, the link performance and the quality of service (QoS) of FSO systems are affected by the unpredictable atmospheric phenomena, especially turbulence and fog/smoke induced fading. This results in channel impairments and fluctuations of both the amplitude and phase of the propagating optical signals particularly over longer transmission link spans [1]. To overcome this problem, several techniques, including multiple-input multiple-output (MIMO) and relay-assisted FSO systems have been proposed in the literature [4-6]. Among the available techniques, MIMO is a reliable technology to realize spatial diversity and to alleviate the atmospheric turbulence induced fading and fog induced attenuation in long distance data transmissions [2]. However, the fundamental characteristics of MIMO systems imposed challenges such as costly multiple transmitters (Txs) and the receivers (Rxs), as well as the complexity of hardware design

This article has been accepted for publication in a future issue of this journal, but has not been fully edited. Content may change prior to final publication. Citation information: DOI 10.1109/ACCESS.2021.3092968, IEEE Access

and implementation when using high-speed optical devices (i.e., lasers, laser drivers, and photodetectors (PDs) [7].

In OWC, the optical beam can be modulated using either analogue or digital signals, and the evaluation of methods for different applications deserves the flexibility of software-defined radio (SDR). SDR provides a re-usable and future-proof platform by means of combining an RF-to-baseband transceiver physical layer and a digital smart processor. This offers many advantages including (*i*) software-configurability and control; (*ii*) improved system performance with the efficient and flexible use of the RF spectrum to offer available new services to the users; (*iii*) a reduced system size and minimization of the design risk and time-to-market; and (*iv*) flexibility in research and development due to the implementation and verification of a range of newly developed protocols using the RF platform-based testbeds [8], [9]. In [10-12], implementation of a MIMO system deploying universal software radio peripheral (USRP) for synchronization, beamforming in the RF domain using the SDR environment for all digital and low-cost systems were reported.

Highly flexible and powerful SDR platforms to accommodate 5G wireless networks have also been reported in the literature [13-15]. Apart from highly reconfigurable software defined implementation in the RF domain, SDR has also attracted considerable interest in OWC systems for diverse applications. In [16], experimental evaluation and performance analysis of an indoor visible light communications (VLC) system with adaptive software-defined equalization using USRPs and LABVIEW was reported. The work reported validated the flexibility of LABVIEW software platform and the ability to improve the measured data simply by changing the software side of the testing prototype. LiFi systems in the range of visible, infrared (IR), and ultraviolet (UV) bands over a 20 m linkspan using LimeSDR USB and GNU Radio for research and development purposes to perform data transmission between two optical transceivers are also commercially reported [17]. Validation of the IR optical front ends with a bandwidth of 10 MHz for USRPs for transmission of an audio signal was reported in [18].

In this work, we outline the design and implementation of out of tree (OOT) modules/signal processing blocks integrated into GNU Radio. Then we analyse the performance of a MIMO intensity modulation-direct detection FSO system with the adaptive switching using GNU Radio under various atmospheric conditions for real-time data transmission. To the best of the authors' knowledge, the proposed system is the first implementation of MIMO FSO in the SDR platform. We investigate the FSO link in the SDR environment and evaluate its performance in terms of the bit error rate (BER) performance under fog and turbulence conditions using GNU Radio. We show that, the proposed system (i) could effectively operate in heavy fog with a BER within the range of 10^{-8} to ~ 10^{-7}, for the link spans of 100, 200, and 300 m; and (ii) experienced a peak turn-over degradation following switching, with the BER of ~10^{-7} and > 10^{-4} for the moderate and high turbulence levels, respectively over 100 and 200 to 300 m.

The rest of the paper is organised as follows: Sections II and III describe the MIMO FSO system and provide all the design considerations including the adaptive switching mechanisms and implementation of MIMO FSO in the SDR/GNU-Radio environment. Section IV is devoted to the results and discussion on the measured data. Finally, Section V concludes the paper.

II. SYSTEM MODEL

In FSO systems, the link availability as a function of the transmission distance is an important factor, which can vary depending on the applications and geographical areas. Most FSO systems are used in the enterprise market (i.e., the last mile access networks), where, the link availability must meet the five-nine requirements (i.e., 99.999%) [19], [20].

The proposed system with OOT modules facilitates the implementation of N number of Txs and Rxs. In this work we consider a 4 × 2 MIMO FSO system as a proof of concept, see Figure 1. In this design, two sets of Txs and Rxs are used for parallel transmission of two different signals to achieve improved link reliability. A dedicated switching algorithm is proposed to switch on the Tx(s) based on the channel conditions. Each Tx and Rx operates independently or in a unified cluster**.** Fog and turbulence induced attenuation, and geometric losses are considered for assessing the link reliability. The considered key system parameters are given in Table 1. The Tx unit consists of 4-Txs (i.e., Tx-A1, Tx-A2, Tx-B1, and Tx-B2), which are grouped into two clusters of 2-Tx with each cluster transmitting different on-off keying (OOK) data streams i.e., $d_a(t)$ and $d_b(t)$. Note, at the Tx unit within the Tx switch module we have included threshold levels of $L_{\mathrm{Atm(Thres)}}$ and $\sigma^2_{I(\mathrm{Thres})}$ for the fog and atmospheric induced loss and intensity fluctuations, respectively to determine the operation mode using Log-normal and Gamma-Gamma turbulence models [21] [22].

Under normal weather conditions, two independent data streams are transmitted via Tx-A1 and Tx-B1. However, under fog or turbulence, additional Txs (i.e., Tx-A2 and Tx-B2) can be used provided the following conditions i.e., $L_{\mathrm{Atm\,(input)}} \geq L_{\mathrm{Atm\,(Thres)}}$ or $\sigma^2_{I(\mathrm{input})} \geq \sigma^2_{I(\mathrm{Thres})}$ have been met. This is to ensure that the link availability will be maintained as much as possible at the cost of increased transmit power $P_{\mathrm{Tx.}}$ The intensity modulated optical beams are launched into the free space channel using optical lenses. At the Rx side, the received optical beams are focused on to two optical Rxs (i.e., Rx-A and Rx-B), which are composed the PD and trans-impedance amplifiers, via optical collimating lenses. The regenerated electrical signal is then applied to moving average filters, samplers, and threshold detectors (slicers) to recover the estimated version of the transmitted data stream. The bit error rate tester (BERT) is utilized subsequently to compare the received and transmitted data stream to determine the real-time BER. Note, (*i*) the parameters used and the link characteristics in

This article has been accepted for publication in a future issue of this journal, but has not been fully edited. Content may change prior to final publication. Citation information: DOI 10.1109/ACCESS.2021.3092968, IEEE Access

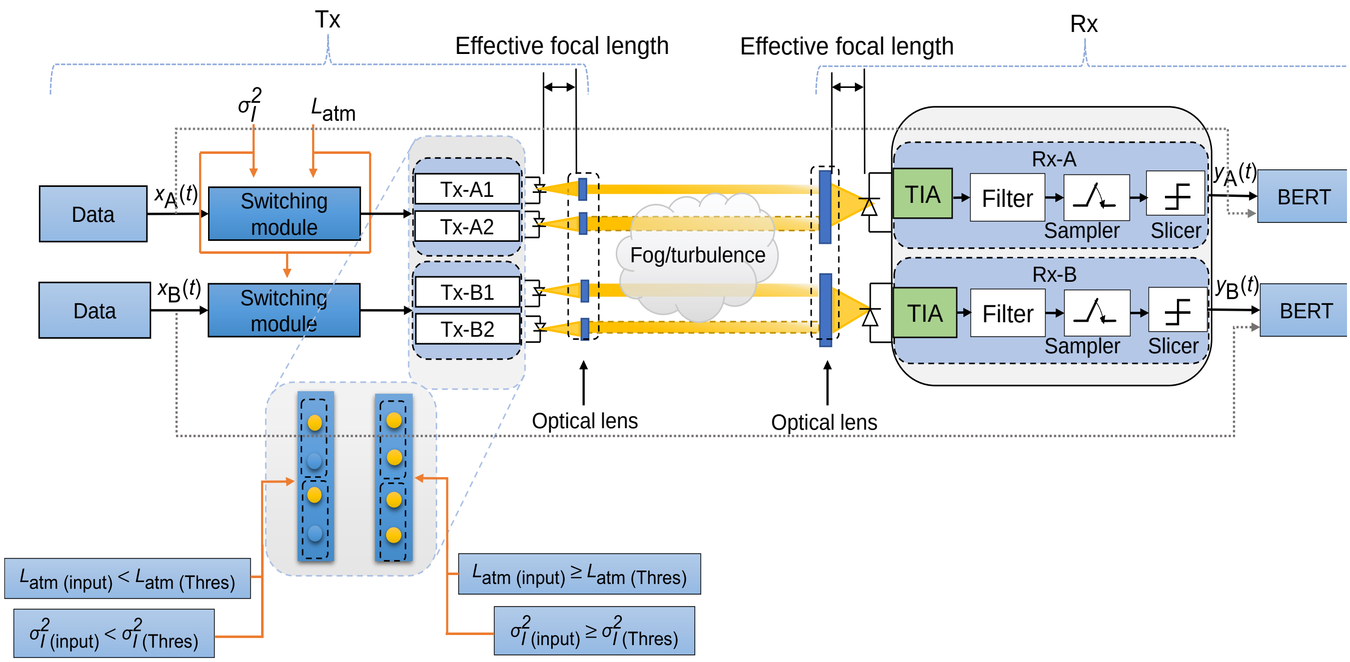

Figure 1. Schematic system block diagram.

terms of the channel loss (visibility V, scintillation index σ_I^2, and refractive index structure parameter C_n^2 for turbulence) are monitored using SDR/GNU Radio; and (*ii*) the extracted link characteristics and the received OOK signal are generated in the GNU Radio software domain.

Table 1. Key System parameters.

Parameter	Value
Link length l	100, 200, 300 m
Number of bits	3.6×10^{10} bits
Transmit power P_{Tx}	10 dBm
Rx lens diameter D_{Rx}	50 mm
Tx lens diameter D_{Tx}	5 mm
Tx beam divergence θ	0.01°
Optical wavelength λ	850 nm
Effective focal length at Rx	~50 mm
Responsivity of PD at 830 nm	0.4 A/W
Rx operating wavelength range	300-1100 nm
Rx bandwidth	30 kHz-1.2 GHz
Noise equivalent power	60 pW/√Hz
Photodetector	PIN
Channel temporal correlation	10 ms
Txs correlation length (for 100, 200 and 300 m)	~1, ~1.3, ~1.6 cm
Tx separation distance d_{Tx}	~7.5 cm
Rx separation distance d_{Rx}	~2.5 cm

A typical FSO system consists of the laser driver, laser source, additional Tx, and Rx optics, PD, and signal processing. Considering the FSO link with no interference, the received signal is given as:

$$y(t) = x(t)\Re \sum_{i=1}^{N_{Tx}} I_i + n(t), \quad (1)$$

where $x(t)$ is the transmitted signal, $\Re$ is the photodetector responsivity and $n(t)$ is the additive white Gaussian noise (AWGN) with variance σ_n^2. $I_i = -\gamma l I_o h_i$ is the received signal intensity from the i^{th} Tx, where I_o is received signal intensity for the ideal channel, h_i is the channel irradiance, l is the link distance, and γ is the weather-dependent attenuation coefficient (in dB/km) typically 0.43, 42.2 for the clear air and moderate fog, respectively [6]. For an FSO link, the channel gain due to the atmospheric conditions is defined by $h_a = e^{-\gamma l}$ [23]. Note, weather attenuation as a function of wavelength λ is given by [24]:

$$\gamma(\lambda) = \alpha_m(\lambda) + \alpha_a(\lambda) + \beta_m(\lambda) + \beta_a(\lambda), \quad (2)$$

where, $\alpha_m(\lambda)$ and $\alpha_a(\lambda)$ are the molecular and aerosol absorption coefficients, respectively, and $\beta_m(\lambda)$ is the molecular scattering coefficient. The last term represents the aerosol scattering coefficient due to fog attenuation which is provided to the Tx switch unit in the proposed system and is expressed as [24]:

$$\beta_a(\lambda) = \frac{3.91}{V}\left(\frac{\lambda}{550\text{ nm}}\right)^{-q}, \quad (3)$$

IEEE Access
Multidisciplinary | Rapid Review | Open Access Journal

where, q is the size distribution of scattering fog particles for which Kruse model is considered in this paper, as given by [25]:

$$q = \begin{cases} 1.6 & V > 50 \text{ km} \\ 1.3 & 6 \text{ km} < V < 50 \text{ km} \\ 0.16V + 0.34 & 1 \text{ km} < V < 6 \text{ km}. \\ V - 0.5 & 1 \text{ km} < V < 1 \text{ km} \\ 0 & V < 0.5 \text{ km} \end{cases} \quad (4)$$

The received power can be expressed as a function of P_{Tx} and the system losses, which is given by:

$$P_{\text{Rx}} = 10^{\frac{L_{\text{Geo}}}{10}} \times 10^{\frac{L_{\text{Atm}}\frac{l}{1000}}{10}} \times 10^{\left(\frac{L_{\text{Misc}}}{10}\right)} P_{\text{Tx}}, \quad (5)$$

where L_{Misc} is the miscellaneous loss including the coupling losses (i.e., optics to fibre). The geometric and atmospheric losses are given, respectively by [26], [27]:

$$L_{\text{Geo}}(\text{dB}) = 20 \log_{10}\left(\frac{D_{\text{rx}}}{D_{\text{tx}} + l \times \theta}\right), \quad (6)$$

$$L_{\text{Atm}}\left(\frac{\text{dB}}{\text{km}}\right) = 4.343\beta_a(\lambda), \quad (7)$$

where D_{tx} and D_{rx} are the Tx and the Rx aperture diameters in meters, respectively and θ is the Tx beam divergence. For varying thermal expansion in the channel, the scintillation index, which is used to estimate the turbulence effect, is given as [28]:

$$\sigma_I^2 = \frac{\langle I^2 \rangle - \langle I \rangle^2}{\langle I \rangle^2}, \quad (8)$$

where $\langle . \rangle$ denotes the ensemble average equivalent to long-time averaging with the assumption of an ergodic process and I is the irradiance of the optical beam. The Rytov variance used for determining the strength of turbulence and is given by [28] :

$$\sigma_R^2 = 1.23 C_n^2 k^{7/6} l^{11/6}. \quad (9)$$

The strength of turbulence can be classified as weak ($\sigma_R^2 < 1$), moderate ($\sigma_R^2 \cong 1$), and strong ($\sigma_R^2 > 1$) [20]. For weak to

Table 2. **The number of Txs used as a function of l, V and L_{Atm} under the fog condition.**

Link length *l* (m)	Visibility *V* (km)	Atmospheric loss L_{Atm} (dB)	Txs used
100	20	0.048	Tx-A1, Tx-B1
	2	0.48	Tx-A1, Tx-B1, Tx-A2, Tx-B2
	1	0.96	Tx-A1, Tx-B1, Tx-A2, Tx-B2
200	20	0.096	Tx-A1, Tx-B1
	5	0.41	Tx-A1, Tx-B1, Tx-A2, Tx-B2
	1	2.7	Tx-A1, Tx-B1, Tx-A2, Tx-B2
300	20	0.14	Tx-A1, Tx-B1
	8	0.36	Tx-A1, Tx-B1, Tx-A2, Tx-B2
	1	4.1	Tx-A1, Tx-B1, Tx-A2, Tx-B2

Table 3. **The number of Txs used as a function of l, σ_I^2 and C_n^2 under the turbulence condition.**

Link length *l* (m)	Scintillation index σ_I^2	Refractive index structure parameter C_n^2 ($m^{-2/3}$)	Txs used
100	5.9×10^{-9}	10^{-20}	Tx-A1, Tx-B1
	0.589	10^{-12}	Tx-A1, Tx-B1, Tx-A2, Tx-B2
	> 1	10^{-11}	Tx-A1, Tx-B1, Tx-A2, Tx-B2
200	2.01×10^{-8}	10^{-20}	Tx-A1, Tx-B1
	0.21	10^{-13}	Tx-A1, Tx-B1, Tx-A2, Tx-B2
	>1	10^{-12}	Tx-A1, Tx-B1, Tx-A2, Tx-B2
300	4.4×10^{-8}	10^{-20}	Tx-A1, Tx-B1
	0.414	10^{-13}	Tx-A1, Tx-B1, Tx-A2, Tx-B2
	>1	10^{-12}	Tx-A1, Tx-B1, Tx-A2, Tx-B2

This article has been accepted for publication in a future issue of this journal, but has not been fully edited. Content may change prior to final publication. Citation information: DOI 10.1109/ACCESS.2021.3092968, IEEE Access

moderate turbulence, we can assume that $\sigma_I^2 = \sigma_R^2$. Note, k is the wave number, and the refractive index structure parameter is expressed as [29]:

$$C_n^2 = \left[79 \times 10^{-6} \frac{P}{T^2}\right] \langle \delta T^2 \rangle r^{-2/3}, \tag{10}$$

where P is the atmospheric pressure in mbar, T is the temperature in Kelvin, and δT refers to the thermal difference between two points separated by a distance r.

Assuming that, the transmitted and received signals of the proposed MIMO FSO system are uncorrelated [30], we numerically calculate the separation space between the Txs and the Rxs, which must exceed the correlation length $d_c \approx \sqrt{\lambda l}$. The correlation coefficient as a function of the separation distance d between the Txs is given by [31]:

$$\rho = \exp\left(\frac{d}{d_c}\right). \tag{11}$$

Using (3), (4), and (7), L_{Atm} is estimated for a range of V from 20 km to 1 km. Using (8) and (9), σ_I^2 is determined for C_n^2 of 10^{-17} to 10^{-11}, which are then adopted in the system simulation to evaluate the link performance in terms of the BER and therefore to determine $L_{\text{Atm(Thres)}}$ and $\sigma_{I(\text{Thres})}^2$, where BER range is ~$10^{-5}$ to ~10^{-3}. For the link with fog and based on the numerically simulated L_{Atm} for a given V and l, selection of the Txs to used is carried out, as outlined in Table 2. Table 3 outlines the number of Txs used under turbulence for the link spans of 100, 200, and 300 m in the MIMO FSO system. Note, σ_I^2 and C_n^2 are estimated to attain the upper limit forward error correction (FEC) BER of 3.8 × 10^{-3}.

III. IMPLEMENTATION OF MIMO FSO IN GNU RADIO/SDR

To investigate the performance of the proposed MIMO FSO system, we have implemented the SDR-based Tx, Rx, and the channel in GNU Radio, as well as a general-purpose processor (GPP)-based real-time signal processing framework. The GNU Radio can also work as a simulation environment without the need for real devices. Note, GNU Radio applications are commonly written in Python language as a package and are combined with digital signal processing (DSP) blocks integrated within GNU Radio and implemented in C++ to perform critical signal processing tasks [32]. Figure. 2 shows the MIMO FSO system implementation in the GNU Radio domain, which is composed of a Tx, a channel, and a Rx.

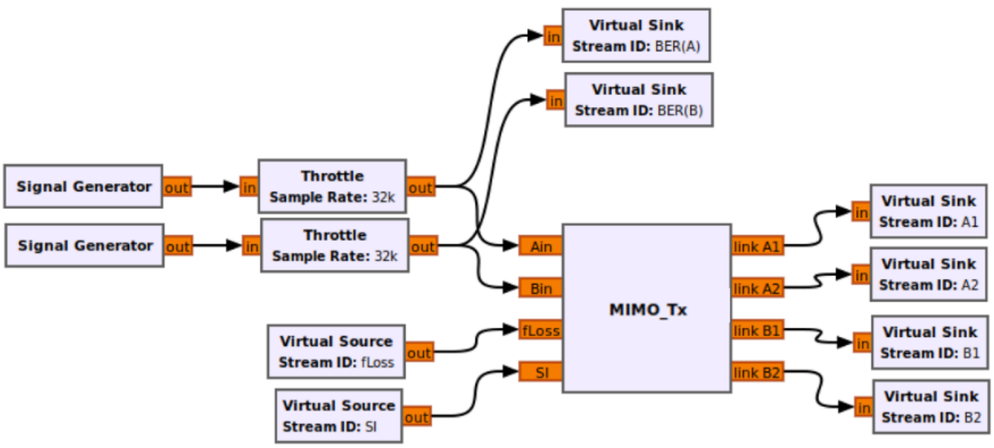

(a)

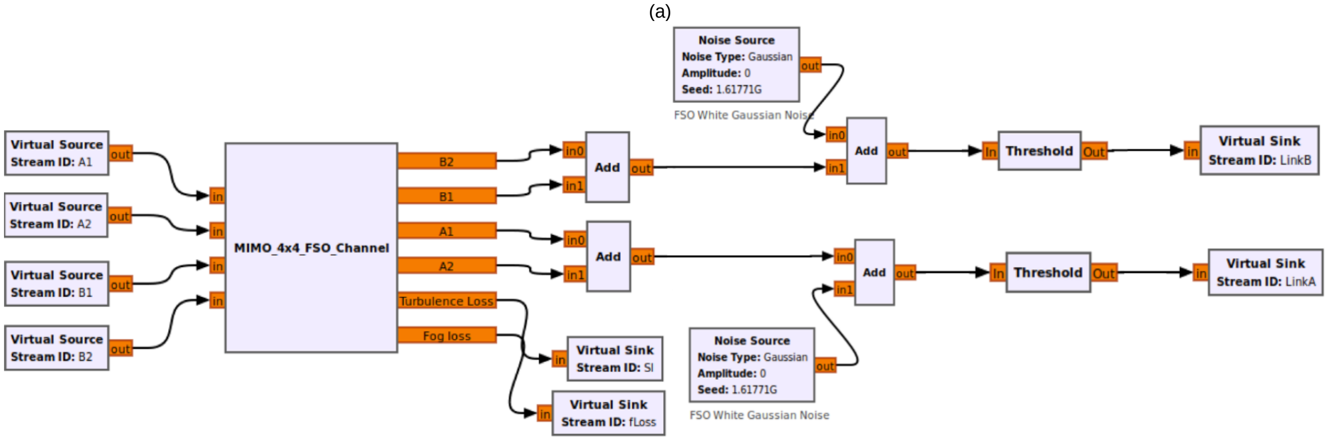

(b)

This article has been accepted for publication in a future issue of this journal, but has not been fully edited. Content may change prior to final publication. Citation information: DOI 10.1109/ACCESS.2021.3092968, IEEE Access

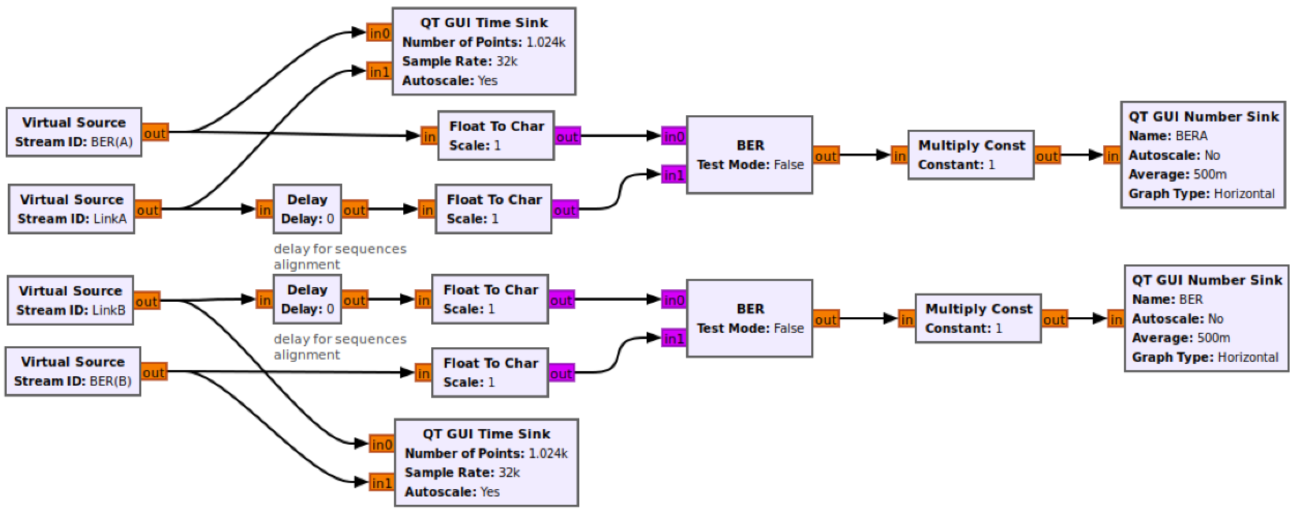

(c)

Figure 2. System implementation for: (a) Tx with fog and turbulence, (b) channel with the additive white gaussian noise, and (c) the Rx with real time BER estimation.

At the Tx, a pseudo random sequence of binary data in the OOK format at the output of the signal generator is applied to the throttle module, which is used to avoid CPU congestion following real time simulation. The outputs of Throttles are applied to (*i*) the virtual sink modules; and (*ii*) the MIMO-Tx module. The output of which are applied to virtual sink modules. In addition, the outputs of the virtual sources, which represent the feedback data on atmospheric loss $L_{\mathrm{Atm\ (input)}}$ in dB and turbulence strength $\sigma^2_{I(\mathrm{input})}$ from the channel, are applied to the MIMO-Tx. The outputs of the

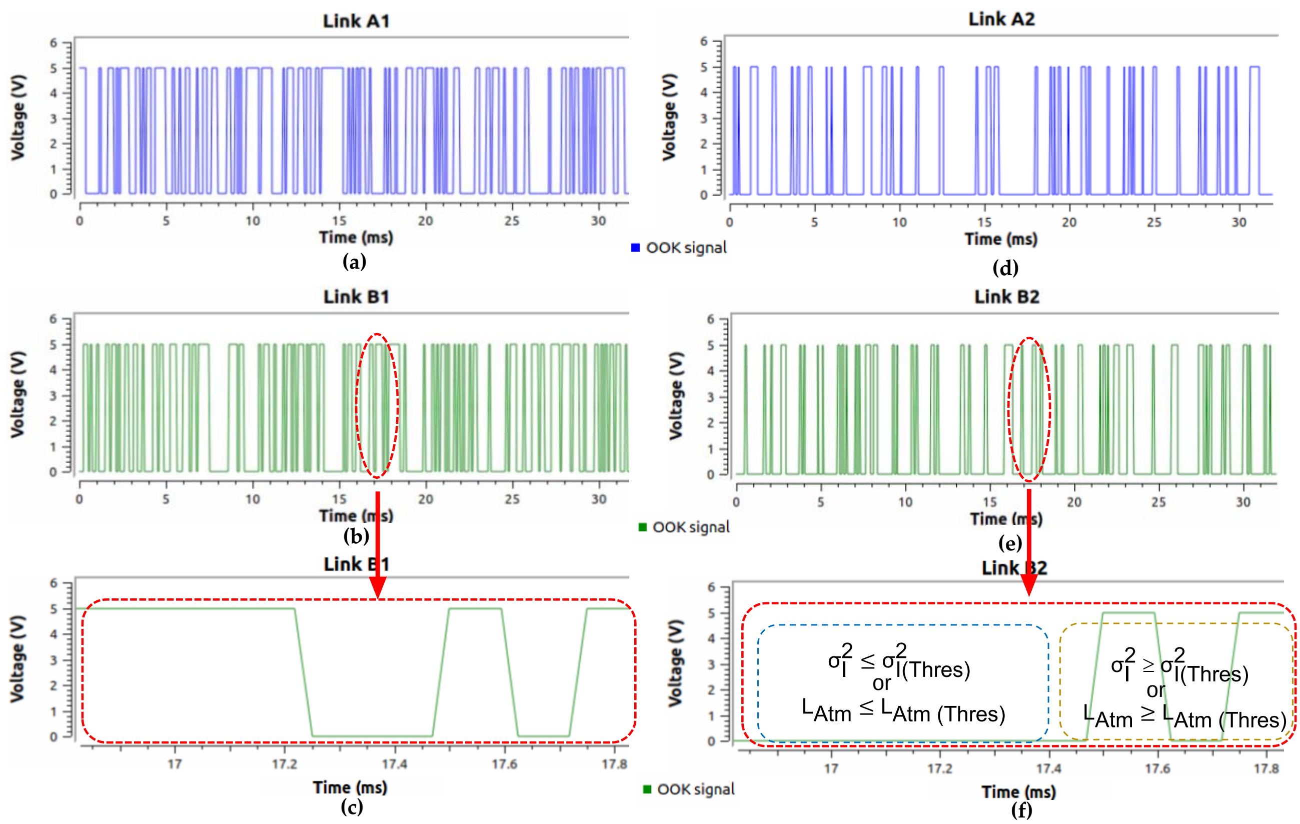

Figure 3. OOK waveforms at the: (a) Tx Link A, (b) Tx link B, (c) optical Rx for a clear channel, and (d) Tx Link A, (e) Tx link B, and (f) optical Rx for an un-clear channel.

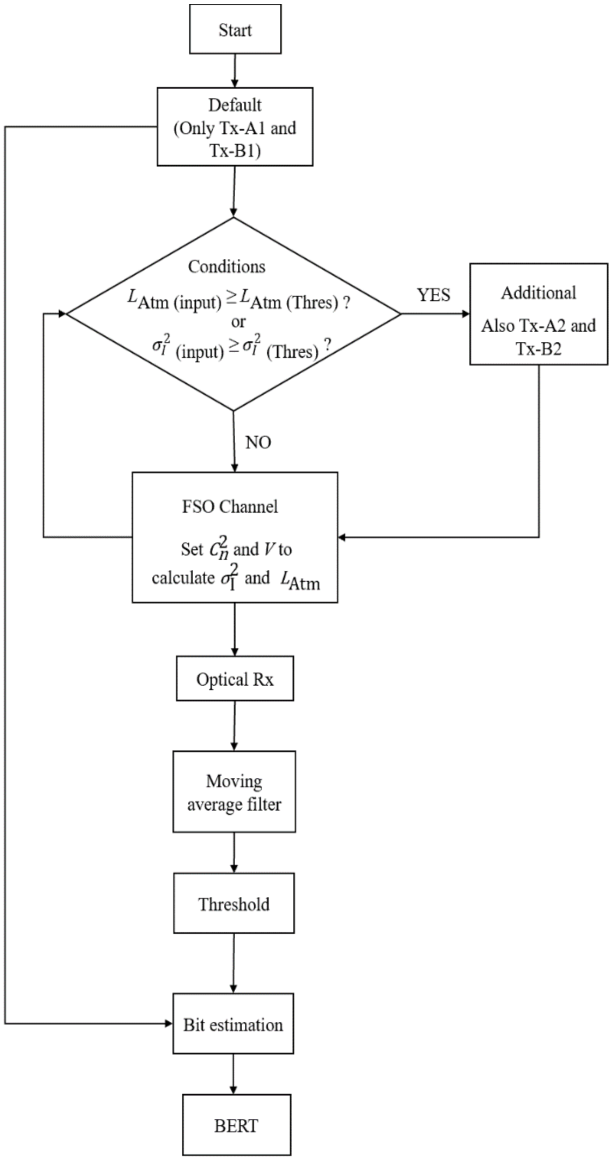

Figure 4. System flow chart.

MIMO-Tx, i.e., Since GNU Radio provides a graphical user interface (GUI) to generate and configure signal processing flow graphs, we have generated sample time waveforms at outputs of the Tx (links A and B), and the optical Rx in Figure 2, as depicted in Figures 3a, b, and c, respectively, under a clear channel, where only single Tx is active at any given time. Depending on the channel condition, provided $L_{\mathrm{Atm}} \geq L_{\mathrm{Atm\,(Thres)}}$ of 0.3 and $\sigma_I^2 \geq \sigma_{I(\mathrm{Thres})}^2$ of 0.02, thus meeting the FEC BER limits of 3.8 $\times 10^{-3}$, additional Txs are switched on to ensure link availability. For this case, the simulated time waveforms are shown in Figure 3d-e.

IV. RESULTS AND DISCUSSION

We have investigated the implementation of MIMO FSO in SDR using the GNU Radio environment. The objective is to monitor and control the proposed system using a software platform without the need for changing the hardware platform and by only updating the software. Implementation of MIMO FSO utilizing the OOT DSP blocks, which is built from scratch, not only satisfies the purpose but also demonstrates real time system performance evaluation. It also has the potential of experimental implementation on the fly due to direct communications with the SDR platform. Here, we have considered a clear channel (i.e., with V of 20 km), P_{Tx} of 10 dBm, 0 dB channel loss, and additional losses including L_{Geo} that are assumed to be low. Using the flow chart shown in Figure 4, we have carried out a simulation to determine the BER as a function of V for single FSO, MIMO FSO, and proposed FSO links with a range of 100, 200, and 300 m under turbulence and fog conditions.

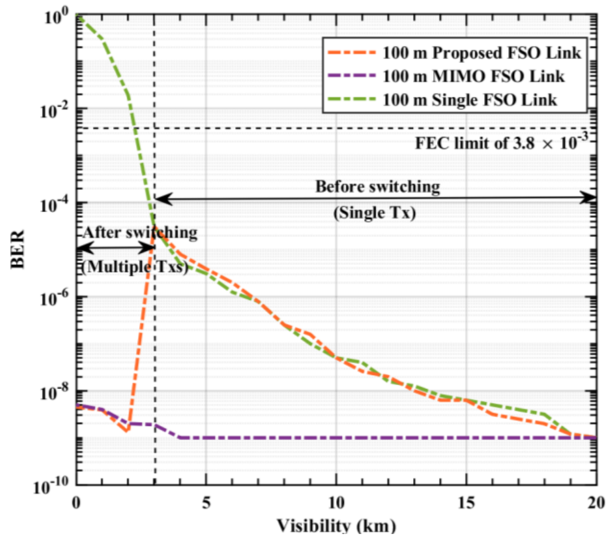

(a)

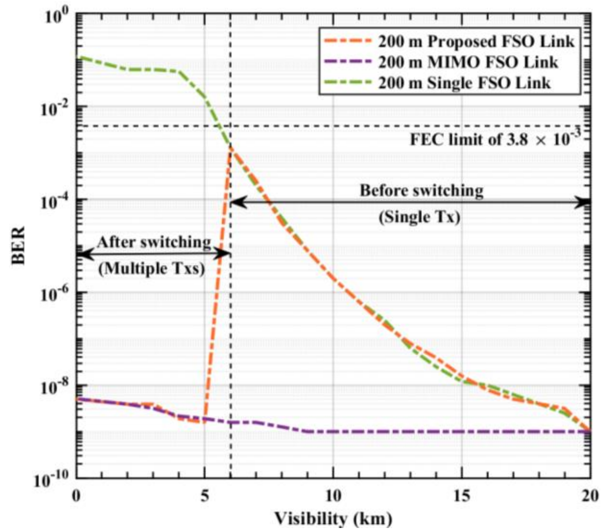

(b)

This article has been accepted for publication in a future issue of this journal, but has not been fully edited. Content may change prior to final publication. Citation information: DOI 10.1109/ACCESS.2021.3092968, IEEE Access

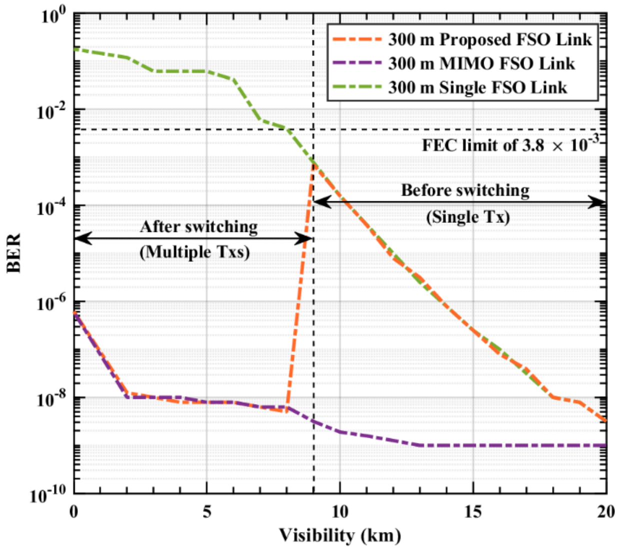

(c)

Figure 5. **BER vs. the visibility for single, MIMO and proposed FSO links of: (a) 100, (b) 200, and (c) 300 m with fog.**

Figure 5 depicts the BER plots for the three systems for the link range of 100, 200, and 300 m under the fog condition. As shown in Figure 5(a), MIMO FSO outperforms the single FSO link for V < 18 km and particularly at lower values of V. At the FEC limit, MIMO FSO meets the BER criteria for all values of V in contrast to the single FSO link where the minimum V is 2 km with BER of 1.9×10^{-2}. For the proposed FSO link, the BER pattern follows the single FSO plot until V of 3km, beyond which the BER drops down to the MIMO FSO link level with BER of ~ 10^{-9}, which is due to turning on additional Txs (i.e., Tx-A2 and Tx-B2) as was explained in the previous section. Note, for the MIMO FSO link, the BER is flat beyond V of 4 km. We observe the same patterns for the BER as in Figure 5 (a), for the 200 and 300 m link as depicted in Figures 5 (b) and (c), except for the switching taking place at V of 6 and 9 km where the BER values are 1.3×10^{-3} and 7.4×10^{-4}, respectively. After turning on additional Txs, BER of the 200 and 300 m proposed FSO links improve to 1.6×10^{-9} at V of 5 km and 5×10^{-9} at 8 km, respectively. Also observed are the BER plot for the MIMO FSO link, which is almost constant (i.e., 10^{-9}) at V > 5 and 10 km in Figures 5 (b) and (c), respectively. calculated Additionally. The beam spot sizes of 17.5 and 34.9 mm in 100 and 200 m, respectively, are smaller, compared to D_{Rx}. Therefore, L_{Geo} is not considered. Due to the beam spot size of 52.4 mm, additional L_{Geo} of 1.2 dB is introduced in 300 m link. to 1.6 $\times 10^{-9}$ at V of 5 km and 5×10^{-9} at 8 km, respectively. Also observed are the BER plot for the MIMO FSO link, which is almost constant (i.e., 10^{-9}) at V > 5 and 10 km in Figures 5 (b) and (c), respectively. calculated Additionally. The beam spot sizes of 17.5 and 34.9 mm in 100 and 200 m, respectively, are smaller, compared to D_{Rx}. Therefore, L_{Geo} is not considered. Due to the beam spot size of 52.4 mm, additional L_{Geo} of 1.2 dB is introduced in 300 m link.

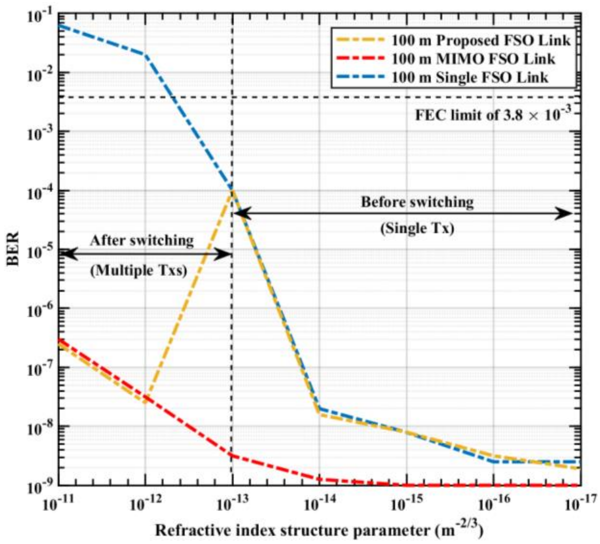

(a)

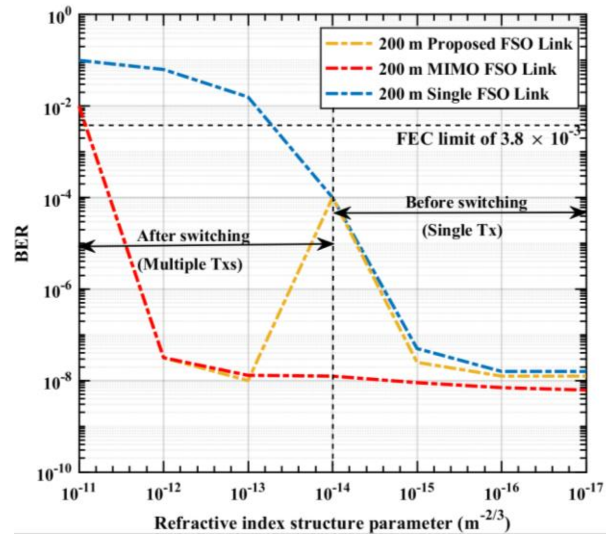

(b)

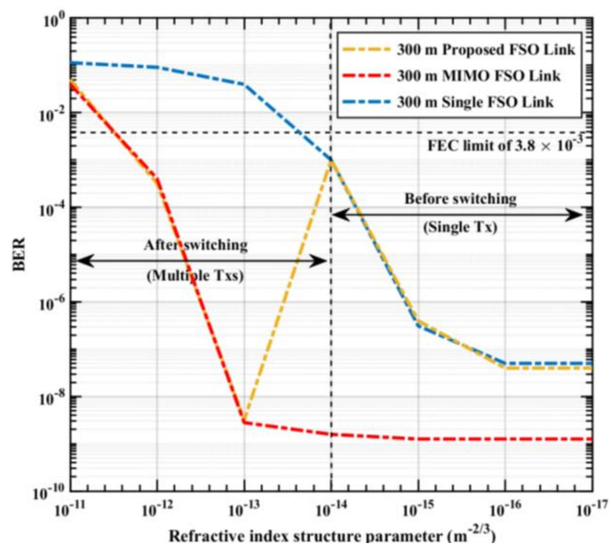

(c)

Figure 6. **The BER against C_n^2 for single, MIMO and proposed FSO links of: (a) 100, (b) 200, and (c) 300 m with turbulence.**

IEEE Access
Multidisciplinary ⋮ Rapid Review ⋮ Open Access Journal

Note that, for all three systems, the estimated BER is above the FEC limit for $\sigma_I^2 < 0.02$, therefore, $\sigma_{I(Thres)}^2$ was set at ≤ 0.02. The systems were then simulated under weak to moderate turbulence (i.e., $10^{-11} < C_n^2 < 10^{-17}$) to determine the BER performance as illustrated in Figure 6 for all three systems and link spans of 100, 200, and 300 m. In these plots, we also observe the same pattern as in Figure 6, with the BER of the 100 m proposed FSO link following the single FSO link plot for C_n^2 of $10^{-13}\text{m}^{-2/3}$, beyond which the BER improves considerably, reaching the level in MIMO FSO link at C_n^2 of 10^{-12} from 10^{-4} to 2.5×10^{-8}, see Figure 6 (a). This improvement in the BER performance is due to switching additional Txs of Tx-A2 and Tx-B2. In Figure 6 (b), the switch-over in the BER plot for the proposed link is at $C_n^2 < 10^{-14}$ dropping down to the BER of 10^{-8} at $C_n^2 < 10^{-13}$ and then increasing with C_n^2. Finally, in Figure 6(c), for the proposed system the BER changes over from 10^{-3} to 3.2×10^{-9} at C_n^2 of 10^{-14} to 10^{-13}, respectively. Note, for (*i*) both MIMO FSO and proposed FSO links the BER floor level is ~ 10^{-9} for $C_n^2 > 10^{-13}$; and (*ii*) the 200 and 300 m long MIMO FSO link performance is deteriorated more under turbulence effects (i.e., $C_n^2 > 10^{-13}$).

V. CONCLUSION

In this work, we have demonstrated a real-time SDR/GNU Radio implementation of a MIMO FSO link with adaptive switching and investigated its performance under different atmospheric conditions. We made the bit-by-bit comparison with the BERT, a signal processing block in GNU Radio. It was shown that, the proposed switching mechanism mitigated the fog and turbulence induced attenuation effectively for range of transmission link spans. We outlined that, the proposed MIMO FSO system with switching technique could effectively operates in heavy fog with a BER within the range of 10^{-8} to ~ 10^{-7} , for the link spans of 100, 200, and 300 m. Additionally, the proposed FSO links experienced a peak turn-over degradation after switching, with BER > 10^{-4} beyond C_n^2 of 10^{-12} in 200 m and 10^{-13} in 300 m respectively, hence, cannot mitigate moderate turbulence effectively, whereas in 100 m link, the proposed system can mitigate moderate turbulence with BER of ~10^{-7}. We concluded that, (*i*) in MIMO FSO, parallel transmission of the same data effectively mitigates fog induced attenuation; and (*ii*) switching on additional Txs overcomes the weak turbulence effect.

REFRENCES

[1] Z. Ghassemlooy, W. Popoola, S. Rajbhandari, *Optical wireless communications: system and channel modelling with MATLAB*. CRC Press; 2 edition (8 April 2019), 2018.

[2] M. Uysal, C. Capsoni, Z. Ghassemlooy, A. Boucouvalas, and E. Udvary, *Optical Wireless Communications : An Emerging Technology* (Signals and Communication Technology). Springer International Publishing, 2016.

[3] Z. Ghassemlooy, S. Arnon, M. Uysal, Z. Xu, and J. Cheng, "Emerging Optical Wireless Communications-Advances and Challenges," *IEEE Journal on Selected Areas in Communications*, vol. 33, no. 9, pp. 1738-1749, 2015, doi: 10.1109/JSAC.2015.2458511.

[4] A. K. Majumdar, Z. Ghassemlooy, and A. A. B. Raj, "Principles and applications of free space optical communications," (in English), 2019. [Online]. Available: https://digital-library.theiet.org/content/books/te/pbte078e.

[5] E. Bayaki, R. Schober, and R. K. Mallik, "Performance analysis of MIMO free-space optical systems in gamma-gamma fading," *IEEE Transactions on Communications*, vol. 57, no. 11, pp. 3415-3424, 2009, doi: 10.1109/TCOMM.2009.11.080168.

[6] N. Mohan, M. M. Abadi, Z. Ghassemlooy, S. Zvanovec, R. Hudson, and M. R. Bhatnagar, "Sectorised base stations for FSO ground-to-train communications," *IET Optoelectronics*, vol. 14, no. 5, pp. 312-318, 2020, doi: https://doi.org/10.1049/iet-opt.2019.0155.

[7] O. Hiari and R. Mesleh, "A Reconfigurable SDR Transmitter Platform Architecture for Space Modulation MIMO Techniques," *IEEE Access*, vol. 5, pp. 24214-24228, 2017, doi: 10.1109/ACCESS.2017.2761859.

[8] L. Xiaolong, H. Weihong, H. Yousefi'zadeh, and A. Qureshi, "A case study of a MIMO SDR implementation," in *MILCOM 2008 - 2008 IEEE Military Communications Conference*, 16-19 Nov. 2008 2008, pp. 1-7, doi: 10.1109/MILCOM.2008.4753441.

[9] M. Arief, S. Mohd Adib, F. Norsheila, Y. Sharifah Kamilah Syed, and R. A. Rashid, "Experimental study of OFDM implementation utilizing GNU Radio and USRP - SDR," in *2009 IEEE 9th Malaysia International Conference on Communications (MICC)*, 15-17 Dec. 2009 2009, pp. 132-135, doi: 10.1109/MICC.2009.5431480.

[10] S. Galih, M. Hoffmann, and T. Kaiser, "Low cost implementation for synchronization in Distributed Multi antenna using USRP/GNU-radio," in *2014 The 1st International Conference on Information Technology, Computer, and Electrical Engineering*, 8-8 Nov. 2014 2014, pp. 457-460, doi: 10.1109/ICITACEE.2014.7065791.

[11] M. M. Rahman, H. E. Baidoo-Williams, R. Mudumbai, and S. Dasgupta, "Fully wireless implementation of distributed beamforming on a software-defined radio platform," presented at the Proceedings of the 11th international conference on Information Processing in Sensor Networks, Beijing, China, 2012. [Online]. Available: https://doi.org/10.1145/2185677.2185745.

[12] F. Quitin, M. M. U. Rahman, R. Mudumbai, and U. Madhow, "Distributed beamforming with software-defined radios: Frequency synchronization and digital feedback," in *2012 IEEE Global Communications Conference (GLOBECOM)*, 3-7 Dec. 2012 2012, pp. 4787-4792, doi: 10.1109/GLOCOM.2012.6503876.

[13] S. Sun, M. Kadoch, L. Gong, and B. Rong, "Integrating network function virtualization with SDR and SDN for 4G/5G networks," *IEEE Network*, vol. 29, no. 3, pp. 54-59, 2015, doi: 10.1109/MNET.2015.7113226.

[14] H. Feng, J. Wu, and X. Gong, "SOUP: Advanced SDR platform for 5G communication," in *2017 IEEE/CIC International Conference on Communications in China (ICCC)*, 22-24 Oct. 2017 2017, pp. 1-5, doi: 10.1109/ICCChina.2017.8330392.

[15] M. Agiwal, A. Roy, and N. Saxena, "Next Generation 5G Wireless Networks: A Comprehensive Survey," *IEEE Communications Surveys & Tutorials*, vol. 18, no. 3, pp. 1617-1655, 2016, doi: 10.1109/COMST.2016.2532458.

[16] Radek Martinek, Lukas Danys and Rene Jaros "Adaptive Software Defined Equalization Techniques for Indoor Visible Light Communication," *Sensors*, vol. 20, no. 6, 2020, doi: https://doi.org/10.3390/s20061618.

[17] H. Technologies. "LiFi R&D Kit." http://www.hyperiontechs.com/lifi-rd-kit/ (accessed 17 Nov 2020, 2020).

[18] H. Boeglen, S. Joumessi-Demeffo, S. Sahuguede, P. Combeau, D. Sauveron, and A. Julien-Vergonjanne, "Optical front-ends for USRP radios," 2018.

[19] I. K. Isaac and J. K. Eric, "Availability of free-space optics (FSO) and hybrid FSO/RF systems," in *Proc.SPIE*, 2001, vol. 4530, doi: 10.1117/12.449800. [Online]. Available: https://doi.org/10.1117/12.449800

[20] M. M. Abadi, Z. Ghassemlooy, N. Mohan, S. Zvanovec, M. R. Bhatnagar, and R. Hudson, "Implementation and Evaluation of a

Gigabit Ethernet FSO Link for 'The Last Metre and Last Mile Access Network'," in *2019 IEEE International Conference on Communications Workshops (ICC Workshops)*, 20-24 May 2019 2019, pp. 1-6, doi: 10.1109/ICCW.2019.8757150.

[21] R. L. P. Larry C. Andrews, *Laser beam propagation through random media* Second Edition ed. Bellingham, Washington 98227-0010 USA SPIE—The International Society for Optical Engineering, 2005.

[22] M. Mansour Abadi, Z. Ghassemlooy, M. R. Bhatnagar, S. Zvanovec, M.-A. Khalighi, and M. P. J. Lavery, "Differential Signalling in Free-Space Optical Communication Systems," *Applied Sciences*, vol. 8, no. 6, p. 872, 2018. [Online]. Available: https://www.mdpi.com/2076-3417/8/6/872.

[23] E. Leitgeb, S. S. Muhammad, C. Chlestil, M. Gebhart, and U. Birnbacher, "Reliability of FSO links in next generation optical networks," in *Proceedings of 2005 7th International Conference Transparent Optical Networks, 2005.*, 7-7 July 2005 2005, vol. 1, pp. 394-401 Vol. 1, doi: 10.1109/ICTON.2005.1505829.

[24] M. K. El-Nayal, M. M. Aly, H. A. Fayed, and R. A. AbdelRassoul, "Adaptive free space optic system based on visibility detector to overcome atmospheric attenuation," *Results in Physics*, vol. 14, p. 102392, 2019/09/01/ 2019, doi: https://doi.org/10.1016/j.rinp.2019.102392.

[25] L. D. M. P. W. Kruse, and R. B. McQuistan, *Elements of Infrared Technology: Generation, Transmission, and Detection* 1963.

[26] E. K. S. Bloom, J. Schuster, and H. Willebrand, "Understanding the performance of free-space optics [Invited]," *J. Opt. Netw. 2*, pp. 178-200, 2003.

[27] R. Paudel, Z. Ghassemlooy, H. Le-Minh, and S. Rajbhandari, "Modelling of free space optical link for ground-to-train communications using a Gaussian source," *IET Optoelectronics*, vol. 7, no. 1, pp. 1-8, 2013, doi: 10.1049/iet-opt.2012.0047.

[28] S. Rajbhandari, Z. Ghassemlooy, P. A. Haigh, T. Kanesan, and X. Tang, "Experimental Error Performance of Modulation Schemes Under a Controlled Laboratory Turbulence FSO Channel," *Journal of Lightwave Technology*, vol. 33, no. 1, pp. 244-250, 2015, doi: 10.1109/JLT.2014.2377155.

[29] H. Kaushal *et al.*, "Experimental Study on Beam Wander Under Varying Atmospheric Turbulence Conditions," *IEEE Photonics Technology Letters*, vol. 23, no. 22, pp. 1691-1693, 2011, doi: 10.1109/LPT.2011.2166113.

[30] S. Zvanovec, J. Perez, Z. Ghassemlooy, S. Rajbhandari, and J. Libich, "Route diversity analyses for free-space optical wireless links within turbulent scenarios," *Opt. Express*, vol. 21, no. 6, pp. 7641-7650, 2013/03/25 2013, doi: 10.1364/OE.21.007641.

[31] M. Abaza, R. Mesleh, A. Mansour, and E. M. Aggoune, "Spatial diversity for FSO communication systems over atmospheric turbulence channels," in *2014 IEEE Wireless Communications and Networking Conference (WCNC)*, 6-9 April 2014 2014, pp. 382-387, doi: 10.1109/WCNC.2014.6952038.

[32] GNURadio. https://wiki.gnuradio.org/index.php/Main_Page (accessed 20/10/2020.

ZUN HTAY received the B.Eng degree in electrical and electronics engineering from Northumbria University, U.K., in October 2019 and later joined the optical communications research group (OCRG) Northumbria University, Newcastle upon Tyne, UK, as a Ph.D. student in October 2019. During her bachelor's degree, Zun obtained the most outstanding student of the department award by IET and awarded by IEEE for her final year project poster presentation. Her PhD is fully funded by the intensive industrial innovation program northeast, United Kingdom (IIIP NE) and is partly funded by the European regional development fund (ERDF) and ISOCOM Ltd.

ZABIH GHASSEMLOOY (Fellow, SOA; Fellow, IET; Senior Member, IEEE; Member, ACM), CEng, BSc (Hons.) in EE Engineering, Manchester Metropolitan Univ., (1981), MSc (1984) and PhD (1987) from Manchester Univ., UK. 1987-88 Post-Doctoral Research Fellow at City Univ., UK. 1988-2004 Sheffield Hallam University, UK, and 2004-14 joined Faculty of Eng. & Env., Northumbria University, UK as an Associate Dean Research, and currently is the Head of Optical Communications Research Group. He is a Research Fellow (2016-) and a Distinguished Professor (2015-) at the Chinese Academy of Science. He was the Vice-Chair of EU Cost Action IC1101 (2011-16) and is Vice- Chair of the EU COST Action CA19111 NEWFOCUS (European Network on Future Generation Optical Wireless Communication Technologies, 2020-2024). He has published 940 papers (373 journals and 8 books), over 100 keynote/invited talks, supervised 10 Research Fellows and 66 PhD students. His research interests are in the areas of optical wireless communications, free space optics, visible light communications, hybrid RF and optical wireless communications with funding from EU, UK Research Council, and industries. He is the Chief Editor of the British Journal of Applied Science and Technology and the International Journal of Optics and Applications, Associate Editor of a number of international journals, and Co-guest Editor of a number of special issues OWC. He is the Vice-Cahir of OSA Technical Group of Optics in Digital Systems (2018-). He is the Chair of the IEEE Student Branch at Northumbria University, Newcastle (2019-). From 2004-06 he was the IEEE UK/IR Communications Chapter Secretary, the Vice-Chairman (2006-2008), the Chairman (2008-2011), and Chairman of the IET Northumbria Network (Oct 2011-2015).

MOJTABA MANSOUR ABADI received the B.Sc. degree in electrical engineering from Islamic Azad University, Fasa, Iran, in 2005, and the M.Sc. degree in electromagnetic fields and waves from the K.N. Toosi University of Technology, Tehran, Iran, in 2008. In 2016, he received his Ph.D degree in optical communication from the optical communications research group (OCRG), Northumbria University, Newcastle upon Tyne, UK. He is currently a lecturer in Mathematics, Physics, and Electrical Engineering department at Northumbria university. His research interest is mainly focused on optical devices, optics, electronics and optics prototyping, terrestrial optical communications, and space optical communications.

ANDREW BURTON received his B.Eng(Hons), M.Sc and Ph.D. degrees from the faculty of Engineering and Environment, Northumbria University, Newcastle U.K. in 2007, 2008 and 2015 respectively. Following the Ph.D., he served as a post doctorial researcher with the renowned optical communications research group (OCRG) working with organic LEDs for optical communications. Andrew has published over 50 scholarly articles in the field of optical communications, with the majority in upper quartile publications. He is currently the technical manager at Isocom Ltd. where they build and test opto-electronic components for the space, military, and commercial sectors. His research interests are focused on optical communications, digital signal processing and opto-electronic systems.

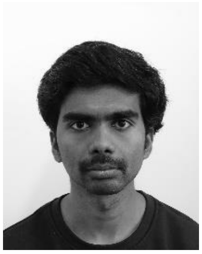

NITHIN MOHAN received his B.Tech degree in electrical and electronics engineering from Amrita School of Engineering Bangalore, India in 2013, and MSc. degree in embedded microelectronics and wireless systems in 2018. He is currently a part of the optical communications research group (OCRG) pursuing his PhD under the supervision of Prof. Fary Ghassemlooy. He has two years industrial experience as a software developer for IBM India. His research interests include free space optical communication, Forward error correction, Software defined radio and software defined networks.

STANISLAV ZVANOVEC received his M.Sc. and Ph.D. degrees from the Faculty of Electrical Engineering, Czech Technical University (CTU) in Prague, in 2002 and 2006, respectively. He is currently working as a Full Professor, the Deputy Head of the Department of Electromagnetic Field and head of Wireless and Fiber Optics at CTU (optics.elmag.org). His current research interests include free space optical, visible light communications and fiber optical systems, OLED based technologies and RF over optics. He is the author of two books (and co-author Visible Light Communications: Theory and Applications), several book chapters and more than 300 journal articles and conference papers.